Two-Dimensional MXene with Controlled Interlayer Spacing for Electrochemical Energy Storage

Patrice Simon

Two-Dimensional MXene with Controlled Interlayer Spacing for Electrochemical Energy Storage

Patrice Simon*,†,‡

†Université Paul Sabatier, CIRIMAT UMR CNRS 5085, 118 route de Narbonne, 31062 Toulouse, France
‡Réseau sur le Stockage Electrochimique de l'Energie (RS2E), FR CNRS 3459, 33 rue Saint Leu, 80039 Amiens, France

ABSTRACT: In this issue of *ACS Nano*, Luo *et al.* report the preparation of pillared two-dimensional (2D) Ti_3C_2 MXenes with controllable interlayer spacings between 1 and 2.708 nm. These materials were further intercalated by ion exchange with Sn(+IV) ions. The results show improved electrochemical performance due to improved ion accessibility into the 2D structure as well as the confinement effect, which limits volume expansi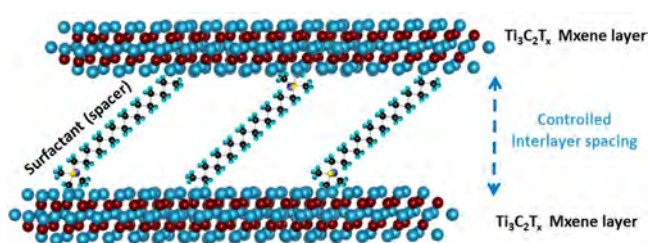on during the Li-alloying reaction. Beyond this specific example, the demonstration that the interlayer spacings of MXenes can be fine-tuned by creating pillared structures based on the spontaneous intercalation of surfactants opens new perspectives in the field of electrochemical energy storage.

Climate change and the decreasing availability of fossil fuels require society to move toward sustainable and renewable resources. As a result, recent decades have seen increases in harvesting and utilizing renewable energy from sources like solar energy and wind, as well as the development of low-CO_2 emission hybrid electric vehicles and electric vehicles (EV). The development of these technologies highlights the need for efficient, high-performance electrochemical energy storage (EES) devices to store and to deliver the energy produced from renewable sources.[1] The current generation of commercial Li-ion batteries (LiBs) offers the best performance in terms of energy density, reaching values of 200 Wh·kg^{-1}. Advanced LiBs (using active materials such as Si for the anode or Li-rich materials for the cathode) and new chemistries (Li–sulfur, Li–air) are also under development with the aim of pushing the energy density of LiBs to new heights.[1] Going back to the example of the EV, the energy density of the battery defines the autonomy of the car—how far we can drive—while the power density determines the acceleration rate. Thus, both the energy density and the power density are important performance metrics for EES devices, and there is an inevitable trade-off between the two for batteries. Energy storage in LiBs is achieved through electrochemical Li-ion intercalation, or insertion, into the bulk of microsized active material particles, and the electrochemical potential of the redox couple and the specific capacity (mAh·g^{-1}) define the energy density. Li$^+$ diffusion in the bulk of the solid active material is the rate-limiting step of this electrochemical reaction, and it follows that this process limits the power performance of the cell. Decreasing the diffusion length by reducing the active material particles to the nanoscale has been proposed to improve the intercalation reaction rate and thus the power performance, but this approach has fallen short in most cases, due to the intrinsic reactivity of the nanoparticle surfaces. When using electrode materials with operating potentials close to that of the electrolyte stability potential window, the nanoscale particles drive unwanted decomposition reactions of the electrolyte at a rate much higher than that of their bulk counterparts.[2] Another route for improving the ionic transport inside the materials is to use exfoliated two-dimensional (2D) materials, where most of the surface area of the material is in contact with the electrolyte. Graphene was the first 2D material successfully prepared, but graphene is limited to the chemistry of carbon, does not tap into metal redox reactions, and its conductivity is substantially decreased by the addition of redox-active functional groups. It suffers from low volumetric performance due to low density, as well as restacking issues.[3] Transition metal dichalcogenides (TMDs) such as MoS_2 have been extensively employed as active materials for batteries and supercapacitors. However, their electrochemical performances are mainly limited by their low electronic conductivity, structural instability, or low areal capacity (mAh·cm^{-2}) due to low electrode weight loadings or the use of thin films when employed as raw electrode materials.[4]

MXenes are a novel family of 2D early transition metal carbides, nitrides, and carbonitrides. MXenes are produced by selectively etching the A element from MAX phase ceramic materials with $M_{n+1}AX_n$ chemistries, where "M" is an early transition metal, "A" is an A group element (mostly groups 13 and 14), "X" is carbon or nitrogen, and n = 1, 2, or 3.[5] Immersing MAX phases in HF solutions, or in acidic solutions

containing a fluoride salt like LiF, results in the "A" atoms being selectively etched away. MXenes are usually referred to as $M_{n+1}X_nT_x$, where T represents surface termination groups ($=O$, $-OH$, and/or $-F$) and x is the number of terminating groups per formula unit (see Figure 1).
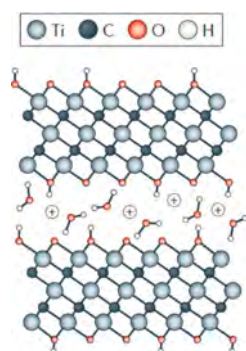

Figure 1. Schematic illustration of cation intercalation between $Ti_3C_2T_x$ layers in aqueous electrolyte; in this example, Ti_3C_2 MXene layers are terminated with OH^- groups. Adapted with permission from ref 6. Copyright 2017 Macmillan Publishers Limited.

MXenes offer key advantages over other 2D materials for energy storage applications. First, the oxygen and/or fluoride groups present at the surface of the $M_{n+1}X_nT_x$ layers weakly bond the individual layers together, resulting in MXenes being susceptible to exfoliation to produce colloidal solutions of single MXene flakes. Also, the rich transition metal chemistry of MXenes enables tuning their electronic properties from metallic to semiconducting, depending on the nature of M, X, and the surface termination groups. For example, OH-terminated Ti_3C_2 is metallic, with electrical conductivity as high as 6500 S·cm^{-1},[6] which is of great importance for designing high-power battery electrodes. Last, MXenes can be used as host materials for the Li-ion intercalation/deintercalation reaction, and capacities up to 280 mAh·g^{-1} at a rate of 1C have been reported for V_2C.[6] During Li-ion intercalation, charge compensation is achieved through the change of the valency of the "M" transition metal in the $M_{n+1}X_nT_x$ layer. However, one of the main concerns of MXenes for Li-ion battery applications lies in the large potential range where the Li-ion intercalation/deintercalation occurs, from ca. 0 to 2 V versus Li$^+$/Li and beyond,[7] which is too great a range for a battery anode material. Since narrowing the potential range would come with a decrease in the delivered capacity, an alternative approach is to combine MXenes with another material that is electrochemically active versus Li ions at lower potential. To achieve this combination, specific synthesis routes have to be developed for designing tailored structures where the active material is entrapped between the MXene layers, thus offering (i) improved ion accessibility to the MXene surface due to an accessible structure and (ii) confinement to limit the volume expansion of the active material during Li-ion intercalation. As an example, such an approach would enable the use of Li-alloying materials, which are known to have extremely high capacity at low potentials but to suffer from significant volume expansion during the alloying reaction, which limits their cycle life.[2]

> MXenes offer key advantages over other 2D materials for energy storage applications.

As described in this issue of ACS Nano, Luo et al. succeeded in preparing pillared Ti_3C_2 MXenes with 10 nm Sn particles between the MXene layers for use as negative electrodes in hybrid devices in combination with activated carbon electrodes.[8] Inspired by the interesting structure of pillared interlayered clays (PILCs), they prepared pillared MXenes, which are "highly conductive clays", via a facile liquid-phase prepillaring and pillaring method. Figure 2 shows a schematic illustration of
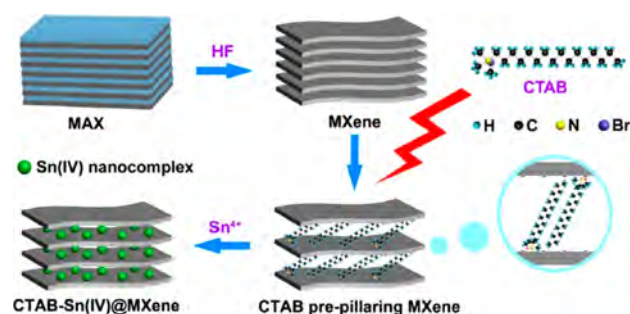

Figure 2. Schematic illustration of preparation of CTAB−Sn(IV)@ Ti_3C_2 by HF etching, CTAB prepillaring, and Sn^{4+} pillaring methods. Reprinted from ref 8. Copyright 2017 American Chemical Society.

the preparation of Ti_3C_2 MXene containing Sn(+IV)-complexed ions, labeled as CTAB-Sn(+IV) Ti_3C_2. The synthesis was achieved in two different steps.[8] First, they prepared a prepillared Ti_3C_2 MXene by intercalating cationic surfactants with various lengths of hydrophobic alkyl chains. When Ti_3C_2 was immersed in the cationic surfactant solution, the cationic surfactant was spontaneously self-assembled and intercalated between the negatively charged layers of Ti_3C_2 by electrostatic interactions, causing an increase in the interlayer spacing between Ti_3C_2 layers. Interestingly, they were able to control and to tune the interlayer spacing between Ti_3C_2 layers by playing with the nature of the surfactant used and the alkyl chain lengths, as well as the temperature of the solution. Although the interlayer spacing did not change linearly with the alkyl chain length and the temperature of the surfactant solution, they were able to prepare Ti_3C_2 with controllable interlayer spacings between 1 and 2.708 nm. By comparison, the original interlayer spacing for the unmodified Ti_3C_2 MXene has a value of 0.977 nm.

In a second step, due to the increase of the interlayer spacing, Luo et al. intercalated Sn(+IV) ions between the Ti_3C_2 layers prepillared with cetyltrimethylammonium bromide (CTAB@Ti_3C_2) that had an interlayer spacing of 2.23 nm. After immersion of the CTAB@Ti_3C_2 in a solution of SnCl$_4$, Sn^{4+} was successfully intercalated into the CTAB@Ti_3C_2 by an ion-exchange mechanism with CTA$^+$ groups. The potential energy storage space and the exchangeable organic cation group in the CTAB@Ti_3C_2 were believed to facilitate the selective adsorption of Sn^{4+} to form Ti−OSn bonds at the MXene surface. This was possibly due to the smaller radius of Sn^{4+} (0.069 nm) compared to the interlayer spacing of the CTAB@ Ti_3C_2 (2.230 nm). Transmission electron microscopy images show that Sn is present under a nanosized stannic hydroxide Sn(+IV) complex (about 2−5 nm size particles) uniformly distributed in the host matrix, leading to the CTAB−Sn(IV)@ Ti_3C_2 nanocomposites with Sn contents of 8.4 wt %. The CTAB surfactant not only acts as a spacer between the Ti_3C_2 layers but also impedes the agglomeration of the tin-based nanoparticles. This impedance is of great importance because

the nanosized particles should enable fast Li-alloying reactions. Additionally, the confinement inside the host matrix should limit unwanted side reactions with the electrolyte when used in an electrochemical cell. The electrochemical signature of the CTAB−Sn(IV)@Ti$_3$C$_2$ nanocomposites in Li-containing organic electrolyte shows the two contributions of the alloying reaction between Li and Sn at low potential (between 0 and 1.5 V *vs* Li$^+$/Li) as well as the Li$^+$ intercalation reaction inside the Ti$_3$C$_2$ host MXene phase within the full voltage window (0−3.0 V *vs* Li$^+$/Li). Interestingly, a Sn(IV)@Ti$_3$C$_2$ nano-composite prepared from a non-prepillared Ti$_3$C$_2$ host MXene phase does not show any evidence of a Li-alloying reaction signature, indicating that the non-prepillared raw Ti$_3$C$_2$ MXene has an interlayer spacing that is too small to accommodate Sn(+IV) complex nanoparticles. A remarkable stable capacity of 765 mAh·g^{-1} was obtained after 100 cycles at 0.1 A·g^{-1} despite an important irreversible capacity observed at the first cycle (about 60%). The power performance was also very good, with 600 mAh·g^{-1} delivered at 1 A·g^{-1}, which is about a 2C rate. To exploit their power performance further, Luo *et al.* used the CTAB−Sn(IV)@Ti$_3$C$_2$ nanocomposites as the negative electrodes in Li-ion capacitor (LiC) hybrid devices. Hybrid devices combine a battery electrode together with a capacitive activated carbon electrode, the latter storing charges through ion adsorption onto high surface area, porous carbons. In these devices, the battery electrode (CTAB−Sn(IV)@Ti$_3$C$_2$) brings the energy to the system while the porous carbon electrode delivers high power. By optimizing the electrode mass ratio, and due to the high capacity provided by the Li-alloying reaction with Sn, the potential range of the CTAB−Sn(IV)@Ti$_3$C$_2$ negative electrode was kept between 0.3 and 2 V *versus* Li$^+$/Li during the cycling of the hybrid device. Under these conditions, the operating cell voltage could reach 4 V, with a capacity of 150 mAh·g^{-1} of CTAB−Sn(IV)@Ti$_3$C$_2$ at a 70C discharge rate. The electrochemical performance of the CTAB−Sn(IV)@Ti$_3$C$_2$//activated carbon hybrid device is among the best reported so far. The successful synthesis of pillared MXenes and their further intercalation with Sn-based nanoparticles offer interesting opportunities for EES devices that bridge the gap between batteries and high-power supercapacitors.

> As described in this issue of *ACS Nano*, Luo *et al.* succeeded in preparing pillared Ti$_3$C$_2$ MXenes with 10 nm Sn particles between the MXene layers for use as negative electrodes in hybrid devices in combination with activated carbon electrodes.

PERSPECTIVES AND OUTLOOK

Beyond the specific example of hybrid devices, these results open new research paths for improving the performance of MXenes for supercapacitor and battery applications. So far, MXenes, such as the most studied Ti$_3$C$_2$T$_x$, have demonstrated high volumetric and gravimetric capacitance (about 1000 F·cm^{-3} and 500 F·g^{-1}, respectively) in aqueous electrolyte, such as shown in Figure 3a.[9,10] In these electrolytes, MXenes store charge through fast, reversible redox reactions involving proton intercalation and the resulting change of the valency of the transition metal (Ti, for instance).[11]

Moving from aqueous to organic electrolytes to extend the operating voltage window (and thus the energy density of the system) came with limitations in the electrochemical performance, and lower volumetric and gravimetric capacitances were reported.[12,13] There are multiple reasons for these limitations, but the larger sizes of the charge carrying ions, lower electrolyte conductivity, differences in ion solvation energy, and the loss of proton-induced pseudocapacitance are the main factors responsible for the performance limitations of MXenes in organic systems.[10] The pre-intercalation of MXene layers with organic electrolyte salt from the simple solvent exchange method has already improved the performance in nonaqueous electrolyte (see Figure 3), but the gap in performance is still important.

The demonstration that the interlayer spacing of MXenes can be fine-tuned by creating pillared structures based on the spontaneous intercalation of surfactants opens new opportunities for the field. By carefully selecting the types of surfactant
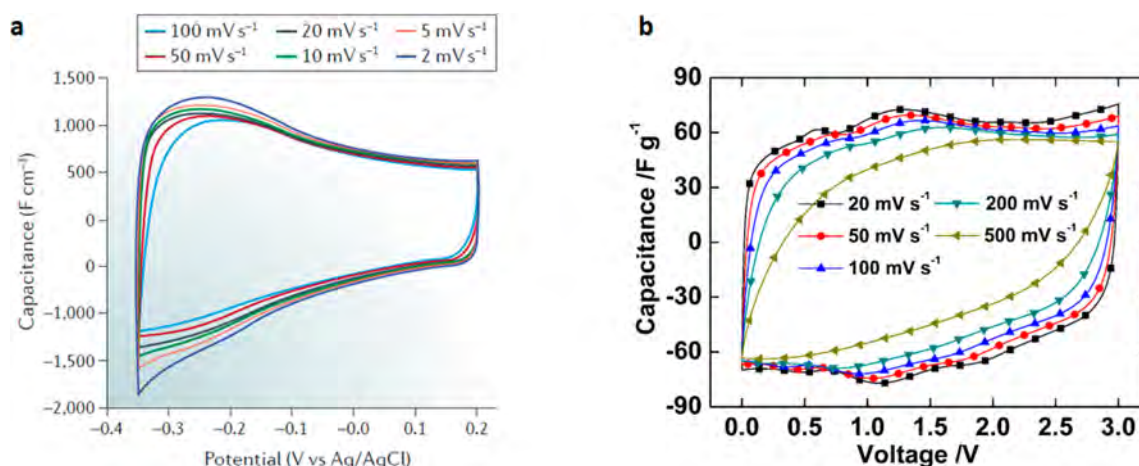

Figure 3. (a) Cyclic voltammograms at different scan rates for a freestanding Ti$_3$C$_2$T$_x$ MXene clay electrode in 1 M H$_2$SO$_4$. Adapted with permission from ref 6. Copyright 2017 Macmillan Publishers Limited. (b) Cyclic voltammograms at different scan rates of a Ti$_3$C$_2$T$_x$ MXene ionogel film in 1-ethyl-3-methylimidazolium bis(trifluoromethylsulfonyl)imide (EMI-TFSI) neat ionic liquid electrolyte. The MXene was pre-intercalated with EMI-TFSI ions before tests using the solvent exchange method to improve ion accessibility to the MXene surface. Adapted with permission from ref 13. Copyright 2016 Elsevier.

molecules, it should be possible to prepare pillared MXene structures with interlayer spacings that match the sizes of the ions of the electrolytes, thus facilitating the adsorption/intercalation of the ions inside the host structure and maximizing the adsorption capacitance, similar to what has been previously demonstrated in porous carbons.[14,15]

In addition, pillared MXenes could be used as model materials for studying the adsorption/intercalation of multivalent ions (e.g., Al^{3+}, Mg^{2+}, Zn^{2+}), which is one of the main challenges in electrochemical energy storage. There is also a need to develop methods for controlling the surface chemistry of MXenes in order to achieve uniform surface terminations for predictable and controllable modification of MXene layers.

The successful development of these approaches would provide guidance for the development of electrode materials for the next generation of batteries and supercapacitors.

AUTHOR INFORMATION

Corresponding Author

*E-mail: simon@chimie.ups-tlse.fr. Tel: +33(0)5.61.55.68.02.

ORCID

Patrice Simon: 0000-0002-0461-8268

Notes

The author declares no competing financial interest.

REFERENCES

(1) Bruce, P. G.; Freunberger, S. A.; Hardwick, L. J.; Tarascon, J.-M. Li–O_2 and Li–S Batteries with High Energy Storage. *Nat. Mater.* **2012**, *11*, 19−29.

(2) Palacin, M. R.; Simon, P.; Tarascon, J.-M. Nanomaterials for Electrochemical Energy Storage: The Good and the Bad. *Acta Chim. Slov.* **2016**, *63*, 417−423.

(3) Ghidiu, M.; Lukatskaya, M. R.; Zhao, M.-Q.; Gogotsi, Y.; Barsoum, M. W. Conductive Two-Dimensional Titanium Carbide 'Clay' with High Volumetric Capacitance. *Nature* **2014**, *516*, 78−81.

(4) Zhang, X.; Hou, L.; Ciesielski, A.; Samori, P. 2D Materials beyond Graphene for High Performance Energy Storage Applications. *Adv. Energy Mater.* **2016**, *6*, 1600671.

(5) Naguib, M.; Kurtoglu, M.; Presser, V.; Lu, J.; Niu, J.; Heon, M.; Hultman, L.; Gogotsi, Y.; Barsoum, M. W. Two Dimensional Nano-Crystals Produced by Exfoliation, of Ti_3AlC_2. *Adv. Mater.* **2011**, *23*, 4248−4253.

(6) Anasori, B.; Lukatskaya, M. R.; Gogotsi, Y. 2D Metal Carbides and Nitrides (MXenes) for Energy Storage. *Nature Rev. Mater.* **2017**, *2*, 16098.

(7) Naguib, M.; Come, J.; Dyatkin, B.; Presser, V.; Taberna, P. L.; Simon, P.; Barsoum, M. W.; Gogotsi, Y. MXene: A Promising Transition Metal Carbide Anode for Lithium-Ion Batteries. *Electrochem. Commun.* **2012**, *16*, 61−64.

(8) Luo, J.; Zhang, W.; Yuan, H.; Jin, C.; Zhang, L.; Huang, H.; Liang, C.; Xia, Y.; Zhang, J.; Gan, Y.; Tao, X. Pillared Structure Design of MXene with Ultralarge Interlayer Spacing for High Performance Lithium ion Capacitors. *ACS Nano* **2017**, xxx DOI: 10.1021/acsnano.6b07668.

(9) Lukatskaya, M. R.; Mashtalir, O.; Ren, C. E.; Dall'Agnese, Y.; Rozier, P.; Taberna, P. L.; Naguib, M.; Simon, P.; Barsoum, M. W.; Gogotsi, Y. Cation Intercalation and High Volumetric Capacitance of Two-Dimensional Titanium Carbide. *Science* **2013**, *341*, 1502−1505.

(10) Hu, M.; Li, Z.; Hu, T.; Zhu, S.; Zhang, C.; Wang, X. High-Capacitance Mechanism for Ti_3C_2Tx MXene by *in Situ* Electro-chemical Raman Spectroscopy Investigation. *ACS Nano* **2016**, *10*, 11344−11350.

(11) Lukatskaya, M. R.; Bak, S. M.; Yu, X.; Yang, X. Q.; Barsoum, M. W.; Gogotsi, Y. Probing the Mechanism of High Capacitance in 2D Titanium Carbide Using *in Situ* X-Ray Absorption Spectroscopy. *Adv. Energy Mater.* **2015**, *5*, 1500589.

(12) Dall'Agnese, Y.; Taberna, P. L.; Gogotsi, Y.; Simon, P. Two-Dimensional Vanadium Carbide (MXene) as Positive Electrode for Sodium-Ion Capacitors. *J. Phys. Chem. Lett.* **2015**, *6*, 2305−2309.

(13) Lin, Z.; Daffos, B.; Taberna, P. L.; Van Aken, K. L.; Anasori, B.; Gogotsi, Y.; Simon, P. Capacitance of Ti_3C_2Tx MXene in Ionic Liquid Electrolyte. *J. Power Sources* **2016**, *326*, 575−579.

(14) Chmiola, J.; Yushin, G.; Gogotsi, Y.; Portet, C.; Simon, P.; Taberna, P. L. Anomalous Increase in Carbon Capacitance at Pore Sizes Less than 1 Nanometer. *Science* **2006**, *313*, 1760−1763.

(15) Galhena, D. T. L.; Bayer, B. C.; Hofmann, S.; Amaratunga, G. A. J. Understanding Capacitance Variation in Subnanometer Pores by *in Situ* Tuning of Interlayer Constrictions. *ACS Nano* **2016**, *10*, 747−754.